

The diluted mixed spin-1/2 and spin-1 Ising model in a transverse random field

N. Benayad, A. Dakhama, A. Fathi and R. Zerhouni

Groupe de Mécanique Statistique des transitions de Phase et Phénomènes Critiques

Laboratoire de Physique Théorique,

Université Hassan II, Faculté des Sciences Ain Chock,

B.P. 5366, Maarif, Casablanca, Morocco.

The diluted mixed spin Ising system consisting of spin-1/2 and spin-1 with a transverse random field is studied by the use of an effective field method within the framework of a single-site cluster theory. The equations are derived using a probability distribution method based on the use of Van der Waerden identities. The phase diagrams are investigated for various lattice structures both for pure and diluted systems, where the transverse field is bimodally and trimodally distributed.

I. INTRODUCTION

Over the last few decades, there has been considerable interest in the theoretical study of the effect of quantum fluctuations in classical spin models. The simplest of such systems is the Ising model in a transverse field. The spin-1/2 transverse Ising model was originally introduced by De Gennes¹ as a valuable model for the tunnelling of the proton in hydrogen-bonded ferroelectrics² such as the KH_2PO_4 type. Since then, it has been successfully applied to several physical systems, such as cooperative Jahn-Teller systems³ (like DyVO_4 and TbVO_4), ordering in rare earth compounds with a single crystal-field ground state,⁴ and also to some real magnetic materials with strong uniaxial anisotropy in a transverse field.⁵ It has been extensively studied by the use of various techniques⁶⁻¹⁰ including the effective field treatment^{11,12} based on a generalized but approximated Callen-Suzuki relation derived by Sà Barreto, Fittipaldi and Zeks. In addition to the works on the two-state spin systems, the spin-one transverse Ising models¹³⁻¹⁹ have received some attention, as well as the quantum transverse spin higher than one.²⁰⁻²⁴

Recently, an other problem of growing interest is associated with the transverse random field Ising model (TRFIM). Special attention has been devoted to bimodal (two peaks) and trimodal distributions for the transverse random field. This model has been investigated using different approximate schemes, such that the mean-field and mean field renormalization group (MFRG),²⁵ a method of combining the MFRG with the discretized path-integral representation (DPIR)^{22,26,27} and an approach combining the pair approximation with DPIR.²⁸ These investigations predicted a discontinuity in the phase diagram at $T=0$, between the bimodal and trimodal random distributions of the transverse field. Using Suzuki-Trotter formula,²⁹ Yokota³⁰ gave arguments which show that the above-mentioned discontinuity at the ground state, seems to be an artifact of the mean-field-like approximation. We point out that all transition lines are second order and the directional randomness of the transverse field does not change the critical behaviour of the system.³⁰

Recently, attention has also been directed to the two-sublattice mixed spin-1/2 and spin-S Ising systems described by the Hamiltonian

$$H = - \sum_{\langle i,j \rangle} J_{ij} \sigma_i^z \sigma_j^z - \sum_i \Gamma_i \sigma_i^x - \sum_j \Gamma_j S_j^x, \quad (1)$$

where σ_i^α and S_j^α ($\alpha=x,z$) are components of spin 1/2 and spin S operators at sites i and j, respectively. J_{ij} is the exchange interaction, Γ_i and Γ_j are transverse fields, and the first summation is carried out only over nearest-neighbour pairs of spins. The Hamiltonian (1) is of interest because it has less translational symmetry than its single spin counterparts. It shows spin reversal symmetry ($\sigma^z \rightarrow -\sigma^z$, $S^z \rightarrow -S^z$, $\sigma^x \rightarrow \sigma^x$, $S^x \rightarrow S^x$) which is spontaneously broken below a field dependent critical temperature. In the absence of the transverse fields ($\Gamma_i = \Gamma_j = 0$), the system is well adapted to study of a certain type of ferrimagnetism.³¹ It has been shown that the $\text{MnNi(EDTA)} \cdot 6\text{H}_2\text{O}$ complex is an example of a mixed-spin system.³² The mixed spin Ising system in the case of $S=1$, has been studied by renormalization group technique,^{33,34} by high-temperature series expansions,³⁵ by free-fermion approximation³⁶ and by finite cluster approximation.³⁷ The effects of dilution on the phase diagrams of these kind of systems are also investigated performing various techniques.^{34,37,38} On the other hand, the influence of the transverse field on the transition temperature have been investigated by using different approximate schemes, such as the effective-field theory based on approximated^{23,39} and exact generalised Van der Waerden identity,^{24,40,41} discretized path-integral representation,¹⁹ and the two-spin cluster approximation.¹⁹

In this work⁴² we are interested in the site diluted mixed spin Ising model in a random transverse field. This system can be described by (1) in which we introduce the site occupancy number ξ_i which takes 0 or 1 depending on whether the site is occupied or not, and a probability distribution function $Q(\Gamma_i)$ for the random transverse field Γ_i . Thus, the Hamiltonian of such system takes the form

$$H = - \sum_{\langle i,j \rangle} J_{ij} \xi_i \xi_j \sigma_i^z \sigma_j^z - \sum_i \Gamma_i \xi_i \sigma_i^x - \sum_j \Gamma_j \xi_j S_j^x. \quad (2)$$

In the present work, we limit our study to the case $S=1$. The transverse fields Γ_i are assumed to be independent variables and obey to trimodal probability distribution

$$Q(\Gamma_i) = p\delta(\Gamma_i) + \frac{1-p}{2}[\delta(\Gamma_i - \Gamma) + \delta(\Gamma_i + \Gamma)], \quad (3)$$

where the parameter p measures the fraction of spins in the system not exposed to the transverse field Γ . When $p=1$ or $\Gamma=0$, the system reduces to the simple diluted mixed spin-1/2 and spin-1 Ising model.

We first investigate the phase diagrams of the mixed spin-1/2 and spin-1 in a transverse random field which is bimodally ($p=0$) and trimodally ($p \neq 0$) distributed. To this end, we use an effective field method within the framework of a single-site cluster theory.⁴³ The effective field equations are derived using a probability distribution method based on the use of generalised Van der Waerden identities⁴⁴ that account exactly for the single-site kinematic relations. Second, we examine the effects of the site dilution on the obtained critical ferromagnetic frontiers. Since the derived state equations are applicable for arbitrary coordination number, phase diagrams are given when the lattice is chosen to be honeycomb, square and simple cubic one.

The outline of this work is as follows: In Section 2, we describe the effective field theory based on a probability distribution method. In Section 3, the phase diagrams of the undiluted and diluted systems are examined and discussed. Finally, we comment our results in Section 4.

II. THEORETICAL FRAMEWORK

The theoretical framework we adopt in the study of the transverse mixed spin-1/2 and spin-1 Ising model described by the Hamiltonian (2), is the effective field theory based on a single-site cluster theory. In this approach, attention is focused on a cluster consisting of just a selected single spin, labelled 0, and the neighbouring spins with which it directly interacts. To this end, the total Hamiltonian given by (2) is rewritten as $H=H_0+H'$, where H_0 includes all terms of H associated with the lattice site 0, namely

$$H_0^\sigma = - \left(\sum_j J_{0j} \xi_0 \xi_j S_j^z \right) \sigma_0^z - \Gamma_0 \xi_0 \sigma_0^x, \quad (4)$$

$$H_0^S = - \left(\sum_i J_{0i} \xi_0 \xi_i \sigma_i^z \right) S_0^z - \Gamma_0 \xi_0 S_0^x, \quad (5)$$

if the lattice site 0 belongs to σ or S -Sublattice, respectively.

First, the problem consists in evaluating the longitudinal and transverse components of the sublattice magnetisation and its quadrupolar moments. Following Sà Barreto, Fittipaldi and Zeks,¹¹ and Sà Barreto and Fittipaldi,¹² the starting point of our approach, in the framework of the single-site cluster theory, is the set of the following identities

$$\langle \sigma_0^\alpha \rangle = \left\langle \frac{\text{Tr}_{\sigma_0} \sigma_0^\alpha \exp(-\beta H_0^\sigma)}{\text{Tr}_{\sigma_0} \exp(-\beta H_0^\sigma)} \right\rangle, \quad (6)$$

and

$$\langle (S_0^\alpha)^n \rangle = \left\langle \frac{\text{Tr}_{S_0} (S_0^\alpha)^n \exp(-\beta H_0^S)}{\text{Tr}_{S_0} \exp(-\beta H_0^S)} \right\rangle, \quad (7)$$

where $\beta=1/k_B T$, $\alpha=x$ or z specifies the components of the spin operators σ_i^α and S_j^α , and $n=1$ and 2 correspond to the magnetisation and the quadrupolar moment, respectively. Tr_{σ_0} (or Tr_{S_0}) means the partial trace with respect to the σ -Sublattice site 0 (or S -Sublattice site 0) and $\langle \dots \rangle$ denotes the canonical thermal average.

The equations (6) and (7) neglect the fact that H_0 and H' do not commute. Therefore, they are not exact for an Ising system in a transverse field. Nevertheless, they have been successfully applied to a number of interesting transverse Ising systems. We emphasise that in the Ising limit $\Gamma_i=0$ for all i , the Hamiltonian contains only σ_i^z and S_j^z . Then, relations (6) and (7) become exact identities.

One notes that since H_0^σ and H_0^S depend on ξ_0 ($\xi_0=0$ or 1), Eqs. (6) and (7) can be written in the

$$\langle \sigma_0^\alpha \rangle = \frac{1-\xi_0}{2\sigma+1} \text{Tr}_{\sigma_0} (\sigma_0^\alpha) + \xi_0 \left\langle \frac{\text{Tr}_{\sigma_0} \sigma_0^\alpha \exp(-\beta \bar{H}_0^\sigma)}{\text{Tr}_{\sigma_0} \exp(-\beta \bar{H}_0^\sigma)} \right\rangle, \quad (8)$$

$$\langle (S_0^\alpha)^n \rangle = \frac{1-\xi_0}{2S+1} + \xi_0 \left\langle \frac{\text{Tr}_{S_0} (S_0^\alpha)^n \exp(-\beta \bar{H}_0^S)}{\text{Tr}_{S_0} \exp(-\beta \bar{H}_0^S)} \right\rangle, \quad (9)$$

which imply

$$\langle \xi_0 \sigma_0^\alpha \rangle = \xi_0 \left\langle \frac{\text{Tr}_{\sigma_0} \sigma_0^\alpha \exp(-\beta \bar{H}_0^\sigma)}{\text{Tr}_{\sigma_0} \exp(-\beta \bar{H}_0^\sigma)} \right\rangle, \quad (10)$$

$$\langle \xi_0 (S_0^\alpha)^n \rangle = \xi_0 \left\langle \frac{\text{Tr}_{S_0} (S_0^\alpha)^n \exp(-\beta \bar{H}_0^S)}{\text{Tr}_{S_0} \exp(-\beta \bar{H}_0^S)} \right\rangle, \quad (11)$$

where

$$\bar{H}_0^\sigma = - \left(J \sum_j \xi_j S_j^z \right) \sigma_0^z - \Gamma_0 \sigma_0^x,$$

and

$$\bar{H}_0^S = - \left(J \sum_i \xi_i \sigma_i^z \right) S_0^z - \Gamma_0 S_0^x.$$

Now we have to evaluate the partial traces on the right-hand side of (10) and (11) over the states of the selected spin, labelled 0. To do this, one can either first find the eigenvalues and eigenstates of \bar{H}_0^σ and \bar{H}_0^S in a representation in which σ^z and S^z are diagonal, or more conveniently one makes use of a coordinate rotation¹⁶ which brings the Hamiltonians \bar{H}_0^σ and \bar{H}_0^S into diagonal forms. For \bar{H}_0^S , the latter method proves the simplest to use. For a fixed configuration of the site occupational numbers ξ_i and transverse fields Γ_i , we obtain

$$\langle \xi_0 \sigma_0^\alpha \rangle = \xi_0 \langle f^\alpha(E_S, \Gamma_0) \rangle, \quad (12)$$

$$\langle \xi_0 (S_0^\alpha)^n \rangle = \xi_0 \langle F_n^\alpha(E_\sigma, \Gamma_0) \rangle, \quad (13)$$

with

$$f^z(E_S, \Gamma_0) = \frac{E_S}{2E_1} \tanh\left(\frac{E_1}{2}\right), \quad (14)$$

$$F_1^z(E_\sigma, \Gamma_0) = \frac{E_\sigma}{E_2} \frac{2 \sinh(E_2)}{1 + 2 \cosh(E_2)}, \quad (15)$$

$$F_2^z(E_\sigma, \Gamma_0) = \frac{1}{(E_2)^2 (1 + 2 \cosh(E_2))} ((\beta \Gamma_0)^2 +$$

$$+ (2(E_\sigma)^2 + (\beta\Gamma_0)^2) \cosh(E_2) \Big), \quad (16)$$

and

$$E_S = \beta \sum_{j=1}^z J_{0j} \xi_j S_j^z, \quad E_1 = ((E_S)^2 + (\beta\Gamma_0)^2)^{1/2},$$

$$E_\sigma = \beta \sum_{i=1}^z J_{0i} \xi_i \sigma_i^z, \quad E_2 = ((E_\sigma)^2 + (\beta\Gamma_0)^2)^{1/2},$$

where z is the coordination number of the lattice. The corresponding results for the transverse components $\langle \xi_0 \sigma_0^x \rangle$ and $\langle \xi_0 (S_0^x)^n \rangle$ may be obtained from the longitudinal components by interchanging (E_S/β) and Γ_0 in Eq. (12) and (E_σ/β) and Γ_0 in Eq. (13), respectively. The next step is to carry out the configurational averaging over the site occupational numbers ξ_i , to be denoted by $\langle \dots \rangle_r$.

In order to perform the thermal and configurational averaging on the right-hand side of Eqs. (14)-(16), we expand the functions $f^\alpha(E_S, \Gamma_0)$ and $F^\alpha(E_\sigma, \Gamma_0)$ as finite polynomials of S_j^z and σ_i^z , respectively, that correctly account for the single-site kinematic relations. This can conveniently be done by employing the Van der Waerden operators⁴⁴

$$f^\alpha(E_S, \Gamma_0) = \prod_j O^{(S)}(S_j^z, \xi_j) f^\alpha(E_S, \Gamma_0), \quad (17)$$

$$F_n^\alpha(E_\sigma, \Gamma_0) = \prod_i O^{(\sigma)}(\sigma_i^z, \xi_i) F_n^\alpha(E_\sigma, \Gamma_0), \quad (18)$$

where

$$O^{(\sigma)}(\sigma_i^z, \xi_i) = \left[(\sigma_i^z + \frac{1}{2}) \bar{\delta}_{\xi_i, 1/2} + (-\sigma_i^z + \frac{1}{2}) \bar{\delta}_{\xi_i, -1/2} \right] \times \\ \times [\xi_i \bar{\delta}_{\xi_i, 1} + (1 - \xi_i) \bar{\delta}_{\xi_i, 0}], \quad (19)$$

$$O^{(S)}(S_j^z, \xi_j) = \left[\frac{1}{2} (S_j^z + (S_j^z)^2) \bar{\delta}_{\xi_j, 1} + \right. \\ \left. + \frac{1}{2} (-S_j^z + (S_j^z)^2) \bar{\delta}_{\xi_j, -1} + \frac{1}{2} (1 - (S_j^z)^2) \bar{\delta}_{\xi_j, 0} \right] \times \\ \times [\xi_j \bar{\delta}_{\xi_j, 1} + (1 - \xi_j) \bar{\delta}_{\xi_j, 0}], \quad (20)$$

where $\bar{\delta}_{A,a}$ is a forward Kronecker delta-function substituting any operator A to the right by its eigenvalue a . In order to carry out the thermal and configurational averaging, we have to deal with correlation functions. In this work, we consider the simplest approximation which neglects correlations between quantities pertaining to different sites, but we take exactly account of the correlation between the site disorder and the local configurational-dependent thermal averages of the spin operators⁴⁵ and use the exact identities

$$\langle \langle (1 - \xi_0) (S_0^x)^n \rangle \rangle_r = \frac{1-c}{2S+1} \text{Tr}_0((S_0^x)^n), \quad (21)$$

$$\langle \langle (1 - \xi_0) \sigma_0^x \rangle \rangle_r = \frac{1-c}{2\sigma+1} \text{Tr}_0(\sigma_0^x), \quad (22)$$

which are directly derived from Eqs. (8)-(11). c denotes the average site concentration defined by $c = \langle \xi_i \rangle_r$. Doing this we find

$$\langle \langle f^\alpha(E_S, \Gamma_0) \rangle \rangle_r = \prod_j^z \left[\sum_{S_j^z=-1}^{+1} \sum_{\xi_j=0}^1 P(S_j^z, \xi_j) \right] f^\alpha(E_S, \Gamma_0), \quad (23)$$

$$\langle \langle F_n^\alpha(E_\sigma, \Gamma_0) \rangle \rangle_r = \prod_i^z \left[\sum_{\sigma_i^z=-1/2}^{+1/2} \sum_{\xi_i=0}^1 R(\sigma_i^z, \xi_i) \right] F_n^\alpha(E_\sigma, \Gamma_0), \quad (24)$$

with

$$P(S_j^z, \xi_j) = \sum_{l_1=-1}^{+1} \sum_{l_2=0}^1 a(l_1, l_2) \delta_{S_j^z, l_1} \delta_{\xi_j, l_2}, \quad (25)$$

$$R(\sigma_i^z, \xi_i) = \sum_{k_1=-1/2}^{+1/2} \sum_{k_2=0}^1 b(k_1, k_2) \delta_{\sigma_i^z, k_1} \delta_{\xi_i, k_2}, \quad (26)$$

where

$$a(\pm 1, 1) = \frac{1}{2} (\pm m_{j1}^z + m_{j2}^z), \quad (27)$$

$$a(0, 1) = (c - m_{j2}^z), \quad (28)$$

$$a(1, 0) = \frac{1}{3} (1 - c), \quad (29)$$

$$b(\frac{\pm 1}{2}, 1) = (\frac{c}{2} \pm \mu_i^z), \quad (30)$$

$$b(\frac{\pm 1}{2}, 0) = \frac{1}{2} (1 - c), \quad (31)$$

where

$$\mu_i^z = \langle \langle \xi_i \sigma_i^z \rangle \rangle_r, \quad m_{jn}^z = \langle \langle \xi_j (S_j^z)^n \rangle \rangle_r. \quad (32)$$

Since the transverse field is randomly distributed, we have to perform the random average over Γ_i according to the probability distribution function $Q(\Gamma_i)$ given by Eq. (3). The order parameters μ^α and m_n^α are then defined as $\mu^\alpha = \overline{\mu_i^\alpha}$, $m_n^\alpha = \overline{m_{jn}^\alpha}$, where the bar denotes the transverse random field average. Thus, using the probability distributions, we obtain the following set of coupled equations for μ^α and m_n^α

$$\mu^\alpha = c \sum_{l_1=-1}^{+1} \dots \sum_{l_z=-1/2}^{+1/2} \sum_{\xi_i=0}^1 \dots \sum_{\xi_z=0}^1 \left[\prod_{j=1}^z a(l_j, \xi_j) \right] \times \\ \times \overline{f^\alpha(\xi_1 S_1^z(l_1), \dots, \xi_z S_z^z(l_z); p, \Gamma)}, \quad (33)$$

$$m_n^\alpha = c \sum_{k_1=-1/2}^{+1/2} \dots \sum_{k_z=-1/2}^{+1/2} \sum_{\xi_i=0}^1 \dots \sum_{\xi_z=0}^1 \left[\prod_{i=1}^z b(k_i, \xi_i) \right] \times \\ \times \overline{F_n^\alpha(\xi_1 \sigma_1^z(k_1), \dots, \xi_z \sigma_z^z(k_z); p, \Gamma)}, \quad (34)$$

where μ_i^z and m_{jn}^z in Eqs. (27)-(31) are replaced by μ^z and m_n^z , respectively; and

$$\overline{f^\alpha}(x, p, \Gamma) = \int Q(\Gamma_0) f^\alpha(x, \Gamma_0) d\Gamma_0,$$

$$\overline{F_n^\alpha}(x, p, \Gamma) = \int Q(\Gamma_0) F_n^\alpha(x, \Gamma_0) d\Gamma_0,$$

with $S_j^z(1) = 1$ and $\sigma_i^z(k) = k$. We like to note that these equations can be solved directly by numerical iteration without further algebraic calculations. This treatment has successfully been used in the study of other systems.⁴⁶

Since the total number of loops ($2z$) is relatively large, the combined sums in (33) and (34) extend over large numbers ($[2(2S+1)]^z$ and $[2(2\sigma+1)]^z$, respectively) of terms, leading to quite long computational time, particularly near second-order phase transition. Therefore, it is advantageous to carry out further algebraic manipulations on Eqs. (23) and (24) employing the differential operator technique

$$f^\alpha(E_S, \Gamma_0) = \exp(E_S D_x) f^\alpha(x, \Gamma_0) \Big|_{x=0}, \quad (35)$$

$$F_n^\alpha(E_\sigma, \Gamma_0) = \exp(E_\sigma D_x) F_n^\alpha(x, \Gamma_0) \Big|_{x=0}, \quad (36)$$

or the integral representation

$$f^\alpha(E_S, \Gamma_0) = \int dx \delta(x - E_S) f^\alpha(x, \Gamma_0), \quad (37)$$

$$F_n^\alpha(E_\sigma, \Gamma_0) = \int dx \delta(x - E_\sigma) F_n^\alpha(x, \Gamma_0), \quad (38)$$

with the delta-function

$$\delta(x) = \frac{1}{2\pi} \int dy \exp(iyx). \quad (39)$$

Choosing the differential operator approach, we obtain from Eqs. (33)-(36)

$$\mu^\alpha = c \left[\sum_{l_1=-1}^{+1} \sum_{l_2=0}^1 a(l_1, l_2) \exp(l_1 l_2 \beta J D_x) \right] f^\alpha(x, p, \Gamma) \Big|_{x=0}, \quad (40)$$

$$m_n^\alpha = c \left[\sum_{k_1=-1/2}^{+1/2} \sum_{k_2=0}^1 b(k_1, k_2) \exp(k_1 k_2 \beta J D_x) \right] F_n^\alpha(x, p, \Gamma) \Big|_{x=0}, \quad (41)$$

which can be reduced to

$$\mu^\alpha = c \left[\frac{1}{2} (m_1^z + m_2^z) \exp(\beta J D_x) + \frac{1}{2} (-m_1^z + m_2^z) \exp(-\beta J D_x) + (1 - m_2^z) \right] \times f^\alpha(x, p, \Gamma) \Big|_{x=0}, \quad (42)$$

$$m_n^\alpha = c \left[\left(\frac{c}{2} + \mu^z \right) \exp\left(\frac{\beta J D_x}{2}\right) + \left(\frac{c}{2} - \mu^z \right) \exp\left(-\frac{\beta J D_x}{2}\right) + (1 - c) \right] F_n^\alpha(x, p, \Gamma) \Big|_{x=0}. \quad (43)$$

Using the multinomial expansion, we find

$$\mu^\alpha = c \sum_{n_1=0}^z \sum_{n_2=0}^{z-n_1} 2^{-(n_1+n_2)} C_z^{n_1} C_{z-n_1}^{n_2} (m_1^z + m_2^z)^{n_1} (-m_1^z + m_2^z)^{n_2} \times (1 - m_2^z) f^\alpha(\beta J (n_1 - n_2), p, \Gamma), \quad (44)$$

$$m_n^\alpha = c \sum_{n_1=0}^z \sum_{n_2=0}^{z-n_1} C_z^{n_1} C_{z-n_1}^{n_2} \left(\frac{c}{2} + \mu^z \right)^{n_1} \left(\frac{c}{2} - \mu^z \right)^{n_2} \times (1 - c)^{z-n_1-n_2} F_n^\alpha\left(\frac{\beta J}{2} (n_1 - n_2), p, \Gamma\right), \quad (45)$$

where C_n^p is the binomial coefficient $n!/[p!(n-p)!]$. The iteration process of these equations becomes suitable for the study of the present system even in the vicinity of the critical temperature.

III. RESULTS AND DISCUSSIONS

In this paper we are interested in investigating the phase diagram of the system described by the Hamiltonian (2). At high temperature, the longitudinal magnetisation

moments μ^z and m_1^z are both equal to zero. Below a transition temperature T_C , we have spontaneous ordering ($\mu^z \neq 0$, $m_1^z \neq 0$), while the corresponding transverse magnetizations μ^x and m_1^x are nonzero at all temperatures. To calculate T_C , it is preferable to expand

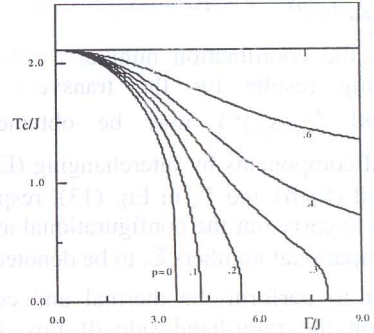


FIG. 1. The phase diagram in T - Γ plane of the mixed spin-1/2 and spin-1 Ising system in a random transverse field on simple cubic lattice ($z=6$). The number accompanying each curve denotes the value of p .

the right-hand sides of (44) and (45) with respect to m_1^z (or μ^z). Doing this we find

$$\mu^\alpha = c \sum_{n_1=0}^z \sum_{n_2=0}^{z-n_1} \sum_{i_1=0}^{n_1} \sum_{i_2=0}^{n_2} 2^{-(n_1+n_2)} C_z^{n_1} C_{z-n_1}^{n_2} C_{n_1}^{i_1} C_{n_2}^{i_2} (-1)^{i_2} \times (m_1^z)^{i_1+i_2} (m_2^z)^{n_1+n_2-i_1-i_2} (1 - m_2^z)^{z-n_1-n_2} \times f^\alpha(\beta J (n_1 - n_2), p, \Gamma), \quad (46)$$

and

$$m_n^\alpha = c \sum_{n_1=0}^z \sum_{n_2=0}^{z-n_1} \sum_{i_1=0}^{n_1} \sum_{i_2=0}^{n_2} C_z^{n_1} C_{z-n_1}^{n_2} C_{n_1}^{i_1} C_{n_2}^{i_2} 2^{-(n_1+n_2+i_1+i_2)} (-1)^{i_2} \times (c)^{n_1+n_2-i_1-i_2} (\mu^z)^{i_1+i_2} (1 - c)^{z-n_1-n_2} \times F_n^\alpha\left(\frac{\beta J}{2} (n_1 - n_2), p, \Gamma\right). \quad (47)$$

For the z -components ($\alpha=z$), they can be written in the following form

$$\mu^z = A_1(\beta J, p, c, \Gamma, m_2^z) m_1^z + B_1(\beta J, p, c, \Gamma, m_2^z) (m_1^z)^3 + \dots, \quad (48)$$

$$m_1^z = A_2(\beta J, p, c, \Gamma) \mu^z + B_2(\beta J, p, c, \Gamma) (\mu^z)^3 + \dots, \quad (49)$$

where A_i, B_i, \dots ($i=1,2$) are obtained from Eqs. (46) and (47) by choosing the appropriate corresponding combinations of indices i_j ($j=1,2$). Retaining only terms linear in μ^z and m_1^z , the second-order transition temperature is then obtained from the equation

$$1 = A_1(\beta J, p, c, \Gamma, m_2^z) A_2(\beta J, p, c, \Gamma), \quad (50)$$

where m_2^z is the solution of the equation (47) for $\mu^z \rightarrow 0$, namely

$$m_{2c}^z = c \sum_{n_1=0}^z \sum_{n_2=0}^{z-n_1} C_z^{n_1} C_{z-n_1}^{n_2} 2^{-(n_1+n_2)} (-1)^{i_2} (c)^{n_1+n_2} \times (1 - c)^{z-n_1-n_2} F_2^z\left(\frac{\beta J}{2} (n_1 - n_2), p, \Gamma\right). \quad (51)$$

A. THE UNDILUTED SYSTEM

First, we study the undiluted case ($c=1$) for the simple cubic lattice ($z=6$). In Fig. 1, we represent the phase diagrams in (T, Γ) plane for various values of p . When the transverse random field is bimodally distributed ($p=0$), the critical temperature decreases gradually from its value $T_C(\Gamma=0)$, to vanish at some critical value $\Gamma_C=3.52$. The phase diagram so obtained is the same as that obtained by two of us (N.B and R.Z)⁴⁷ for the mixed spin-1/2 and spin-1 Ising system in a uniform transverse field. As is shown in the figure, when we consider a trimodal random field distribution (i.e. $p \neq 0$), a finite critical transverse field Γ_C also exists for relatively small values of p . This means that the thermodynamic properties of the system are continuous between the two distributions. We have to point out that the spin-1/2 Ising model in the trimodal random transverse field (3) has been investigated within the standard mean-field and mean-field-like approximations.^{25,28} These studies show a crossover from the trimodal distribution, with $p < 1$, to the bimodal distribution ($p=0$) indicating a discontinuity between these two cases in the ground state phase diagram. Yokota³⁰ discussed this result and, he showed, using the Suzuki-Trotter formula,²⁹ that the above discontinuity may be an artefact of the mean-field-like approximation. In our present work, we have not found a discontinuity in the phase diagram at $T=0$ (see Fig. 1) between the trimodal and the bimodal random field distributions. Thus, our calculations agree with Yokota's conjecture. This is due to the fact that we have used a method which treats correctly all self-spin correlations, while neglecting correlations only between spins on different sites; whereas in the mean-field approximation all correlations are neglected. Moreover, we note the existence of a critical value p^* of p ($p^*=0.478$ for $z=6$)

	T_C/J ($\Gamma=0, c=1$)	Γ_C/J ($p=0, c=1$)	$p^*(c=1)$	$c^*(\Gamma=0)$
$z=3$	0.891	1.42	0.657	0.5378
$z=4$	1.290	2.12	0.600	0.4133
$z=6$	2.111	3.52	0.478	0.2824

Table-1: The critical temperature T_C , the critical transverse field Γ_C , the critical value p^* for the undiluted system, and the percolation threshold c^* for the honeycomb ($z=3$), square ($z=4$) and simple cubic ($z=6$) lattices

indicating two qualitatively different behaviours of the system which depend on the range of p . Thus, for $p < p^*$, the system exhibits at the ground state a phase transition at a finite critical value Γ_C of Γ . But for $p^* < p < 1$, there is no critical transverse field, and therefore, at very low

We note here that the phase diagrams in the case of the

honeycomb ($z=3$) and the square ($z=4$) lattices are qualitatively similar to that plotted in Fig. 1 for the simple cubic lattice. In Table 1, we give the corresponding values of the critical transition temperature T_C when $\Gamma=0$, the critical transverse field Γ_C when $p=0$, and the critical value p^* .

B. THE SITE DILUTED SYSTEM

First, we investigate the system in the absence of the transverse field ($\Gamma=0$ or $p=1$) by solving numerically the Eq. (50). For the simple cubic lattice ($z=6$), the phase diagram is represented in Fig. 2 and it expresses the standard result of a diluted magnetic system.^{37,38} The critical temperature T_C decreases linearly from its value in the mixed Ising system T_C ($c=1$), to reduce rapidly to zero at the percolation threshold $c^*=0.28246$ which is quite good compared with the best value of 0.31 calculated by M. F. Sykes and J. W. Essam.⁴⁸ In table-1, we also give the value of c^* calculated for different coordination number z .

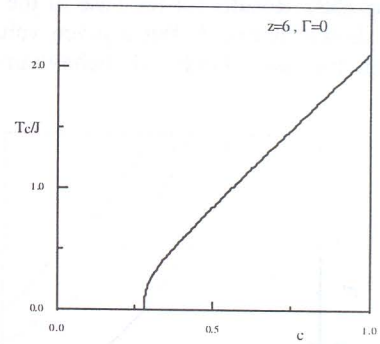


FIG. 2. The phase diagram of the diluted mixed spin-1/2 and spin-1 Ising system on simple cubic lattice ($z=6$) in the absence of the transverse field ($\Gamma=0$, or $p=1$)

Secondly, when the transverse random field is a bimodal distribution ($p=0$), results for the case of the simple cubic lattice are summarised in Fig. 3. These give the sections of the critical surface $T_C(c, \Gamma)$ with planes of fixed values of the dilution parameter c . As is expected

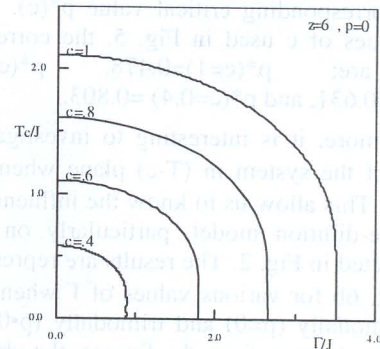


FIG. 3. The phase diagram in T - Γ plane of the diluted mixed spin-1/2 and spin-1 Ising system in a bimodal transverse field ($p=0$), when the value of c is changed from $c=1$ to 0.4.

when $c^* < c < 1$, the general behaviour of the critical

temperature $T_c(c, \Gamma)$ falls with decreasing c and increasing Γ , and vanishes at a critical value Γ_c of the transverse field strength which depends on the value of c . These results have a form similar to those observed in the dilute Ising model in a transverse field.^{49,50}

Next, we investigate the phase diagrams of the system when the form of the random transverse field is chosen to be a trimodal distribution ($p \neq 0$). In the pure system, we have defined a critical value of p , namely p^* above which, at low temperature, the system do not present a finite critical value Γ_c/J which means that the ferromagnetic order is stable for any value of the transverse field Γ . As is expected, such behaviour appears in the diluted case, but the location of p^* depends on the concentration c of magnetic sites. As shown in Fig. 4 for the honeycomb ($z=3$), square ($z=4$), and simple cubic ($z=6$) lattices, p^* increases with decreasing values of c which is physically reasonable. The variation of the critical temperature with the transverse field Γ/J , keeping c and p fixed, is obtained from the Eq. (50). Results for the case of the simple cubic lattice, are shown in Fig. 5. For a given value of c , we have plotted the two kinds of behaviours which have the

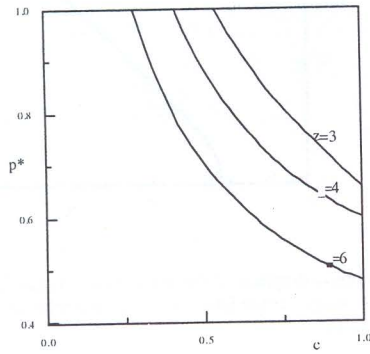


FIG. 4. The dependence of the critical value of p^* as a function of the dilution parameter c , for different lattice structures ($z=3, 4$ and 6).

system when the fraction p of spins not exposed to the transverse field is greater (dashed line) or less (solid line) than the corresponding critical value $p^*(c)$. For the chosen values of c used in Fig. 5, the corresponding p^* values are: $p^*(c=1)=0.478$, $p^*(c=0.8)=0.535$, $p^*(c=0.6)=0.631$, and $p^*(c=0.4)=0.803$.

Furthermore, it is interesting to investigate the phase diagrams of the system in $(T-c)$ plane when Γ and p are kept fixed. This allow us to know the influence of Γ and p on the site-dilution model, particularly on the dilution curve depicted in Fig. 2. The results are represented in Fig. 6a and Fig. 6b for various values of Γ when the random field is bimodally ($p=0$) and trimodally ($p \neq 0$) distributed, respectively. As seen from the figures, the obtained curves have the same shape as the dilution curve, and there appear different thresholds as solutions of the equation $T_c(c, p, \Gamma)=0$. We also note that the critical temperature T_c falls with decreasing c and p , and increasing Γ .

On the other hand, the zero temperature phase diagram for the system under study, is of considerable interest. It is obtained from the solution of the Eq. (50) keeping $T_c=0$.

Fig. 7a shows the dependence of the critical value Γ_c on the concentration c when p takes different values. As is clearly seen from Fig. 7b, the part of the phase diagram near the percolation threshold c^* represents an outstanding feature. In particular, for $p=0$ the critical transverse field Γ_c takes a finite value at $c=c^*$ and shows a discontinuity change from a finite value to zero at $c=0.2637$ below c^* . This result may support the conjecture done by Harris⁸ for the diluted transverse Ising model (DTIM), which can be summarised as follows: at percolation threshold c^* , the critical transverse field should display a discontinuity.

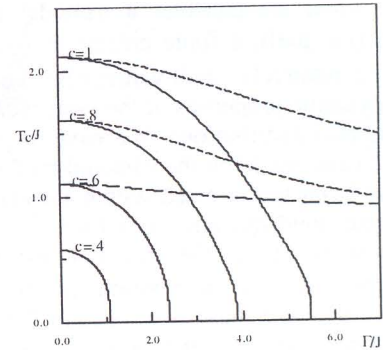


FIG. 5. The phase diagram in $T-\Gamma$ plane of the diluted mixed spin-1/2 and spin-1 Ising system in a random transverse field on simple cubic lattice ($z=6$), when the value of c is changed from $c=1$ to 0.4 , with $p=0.2$ (solid lines), $p=0.6$ (dashed lines), and $p=0.85$ (broken lines).

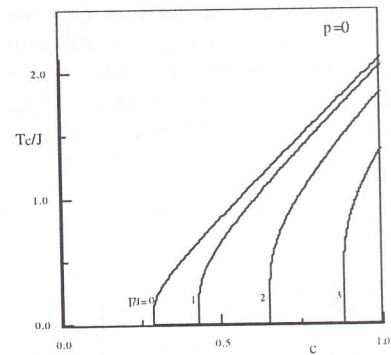


FIG. 6a. The phase diagram in $T-c$ plane of the diluted mixed spin-1/2 and spin-1 Ising system in a random transverse field on simple cubic lattice ($z=6$), with $p=0$ (bimodal distribution). The number accompanying each curve denotes the value of Γ .

It is worthy to notice here that the investigation of the DTIM by series expansion techniques,⁴⁹ CPA treatments, and effective field theory⁵¹ led to a critical transverse field Γ_c which reduces continuously to zero at $c=c^*$. However, the position space renormalisation group methods^{9,52} showed the existence of a discontinuity of Γ_c at $c=c^*$, and therefore they verified the Harris conjecture. On the other hand, when the transverse random field is taken as a trimodal distribution (i.e. $p \neq 0$) Γ_c shows, for a given value of p , a discontinuity similar to that found in the case of bimodal distribution ($p=0$) as shown in Fig. 7b. The discontinuity of Γ_c is located on a (p -dependent) well defined value of c , and its height increases with increasing p . We can also see in Fig. 7b that, for all values of p , the discontinuities appear only in a narrow range of c

($0.2637 < c < c^*$), and at $c=c^*$ the critical field Γ_c takes a finite value which is independent of the value of p .

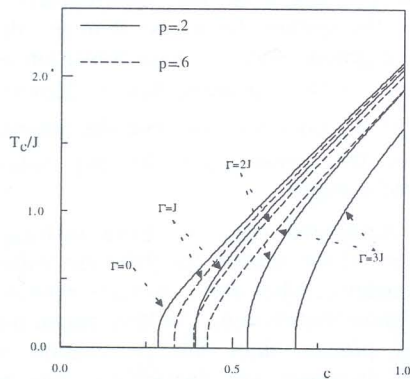


FIG. 6b. The phase diagram in T - c plane of the diluted mixed spin-1/2 and spin-1 Ising system in a random transverse field on simple cubic lattice ($z=6$), with $p=0.2$ (solid lines) and $p=0.6$ (dashed lines). The number accompanying each curve denotes the value of Γ .

Next, let us clarify the role of the applied random transverse field in the diluted mixed spin-1/2 and spin-1 Ising system. To this end, we have examined its

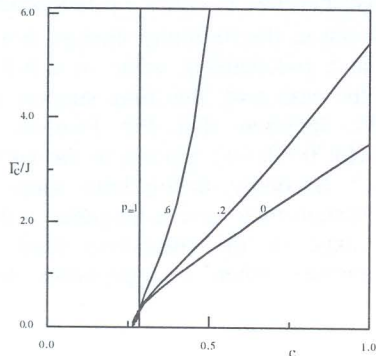


FIG. 7a. The zero temperature phase diagram of the diluted mixed spin-1/2 and spin-1 Ising system in a random transverse field on simple cubic lattice ($z=6$). The number accompanying each curve denotes the value of p .

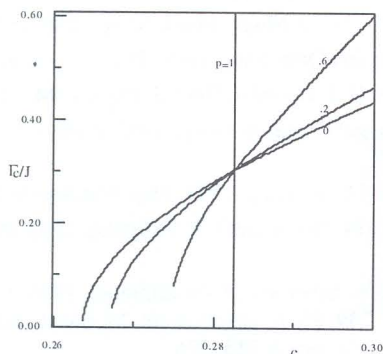


FIG. 7b. The zero temperature phase diagram of the diluted mixed spin-1/2 and spin-1 Ising system in a random transverse field on simple cubic lattice ($z=6$), for different values of p , on an enlarged scale with c in the vicinity of the percolation threshold.

phase diagrams in the (T, Γ) space, selecting two values of c ($c=0.29$ and $c=0.28$) greater and less than the percolation threshold $c^*=0.28246$. For the case of the bimodal distribution ($p=0$), the results are plotted in Fig. 8a. For the system with $c=0.29$, the variation of the critical temperature with the transverse field takes the same form as those depicted in Fig. 3 since $c > c^*$. As shown in the figure, an important behaviour of the system is found with $c=0.28$ (c less than c^*): T_c reduces to zero at $\Gamma=0$ but, however, in a certain range of Γ ($0 < \Gamma < \Gamma_c$) the system exhibits a second order transition at a finite value of T_c which vanishes at $\Gamma = \Gamma_c$. These results indicate that for small transverse field strength, the system may have a magnetic ordering even if c is less than c^* . As seen from Fig. 7b, such behaviour may be obtained in the system when the dilution parameter belongs to the range $0.2637 < c \leq c^*$. On the other hand, when the transverse field is trimodally distributed ($p \neq 0$), the phase diagrams are represented in Fig. 8b for various values of p , when the concentration c takes the above values. Thus, for $c = 0.29$, the T_c curves are plotted for $p=0.2$ and $p=0.99$ which are, respectively, less and greater than its corresponding critical value $p^* = 0.983$ (see Fig. 4). The obtained transition lines have the same shape as those shown in Fig. 5. For the case of $c = 0.28$ the variation of T_c with Γ , for different values of p , are represented in Fig. 8b. They are qualitatively similar to the results (Fig. 8a) obtained for the bimodal distribution when $c < c^*$. In contrast to the case $c > c^*$, we notice that, for a given $c < c^*$ ($c=0.28$ in Fig. 8b), the region which corresponds to the long-range ferromagnetic order, decreases with increasing p and disappears at c -dependent value of p (see Fig. 7b and Fig. 8b). Therefore, when c is less than 0.2637 , there is no magnetic ordering for any values of p and Γ .

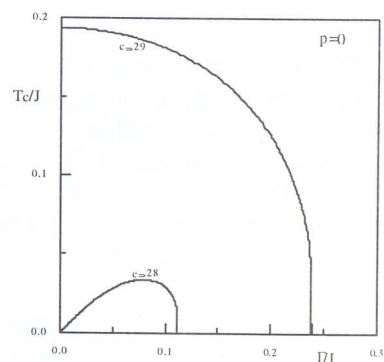


FIG. 8a. The phase diagram of the diluted mixed spin-1/2 and spin-1 Ising system in a bimodal transverse field on simple cubic lattice ($z=6$), when $c=0.29$ and $c=0.28$.

IV. CONCLUSIONS

In this paper, we have studied the undiluted and the diluted mixed spin Ising systems consisting of spin-1/2 and spin-1 in a transverse random field, which is bimodally and trimodally distributed. We have used an effective field method within the framework of a single-site cluster

theory. In this approach, we have derived the equations using a probability distribution method based on the use of Van der Waerden identities accounting exactly for the single-site kinematic relations. We have also included the correlation between the site disorder and the local configurational-dependent thermal average of the spin operators.

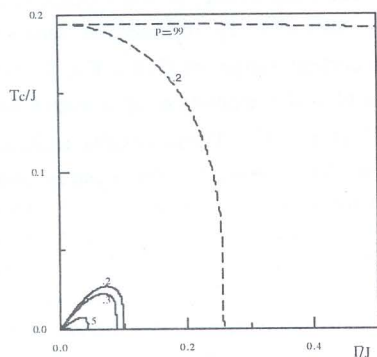


FIG. 8b. The phase diagram of the diluted mixed spin-1/2 and spin-1 Ising system in a random transverse field on simple cubic lattice ($z=6$), when $c=0.29$ (dashed lines) and $c=0.28$ (solid lines) with various values of p .

For the undiluted mixed spin Ising system on simple cubic lattice, we have investigated the variation of the critical temperature T_c with the transverse field Γ for various values of p (p measures the fraction of spins not exposed to Γ). We have not found a discontinuity in the ground state phase diagram between the bimodal (i.e. $p=0$) and trimodal (i.e. $p>0$) random field distributions. This result agrees with Yokota's conjecture.³⁰ It is worthy to note here that the discontinuity found at $T=0$ in the spin-

1/2 Ising models in a transverse random field^{25,28} may be explained³⁰ as an artefact of the used mean-field-like approximations. On the other hand, we have defined a critical value p^* separating two qualitatively different behaviours of the system: for p less than p^* , the system exhibits, at the ground state, a phase transition at a finite critical value Γ_c of the transverse field Γ . However, for p greater than p^* , Γ_c does not exist and the ordered state is stable at very low temperatures for any value of the transverse field strength.

For the site-diluted case, we have investigated the phase diagrams of the system for different values of the dilution parameter c , when the transverse random field is taken as a bimodal distribution. We have found that for the values of c greater than the percolation threshold $c^*=0.2824$, T_c decreases with decreasing c and increasing Γ . When the transverse random field is trimodally distributed, we also have noted (as in the pure case) the existence of the critical value p^* which increases with decreasing values of c . Furthermore, we have plotted the zero temperature phase diagram in Γ_c - c plane for various values of p . Near the percolation threshold, the phase diagrams represent an outstanding features. First, at $c = c^*$ the critical transverse field Γ_c takes a p -independent finite value, and exhibits a discontinuity change from a finite value to zero at a p -dependent value of c below c^* . In particular, for the case $p=0$, this may support the Harris conjecture.⁸ We mention that the location of these discontinuities (for $0 < p < 1$) appears in the narrow range $0.2637 < c < c^*$. Secondly, in this latter range, we have found that the system may have a magnetic ordering in a well defined range of the transverse field, and this behaviour disappears when c approaches to 0.2637.

¹ P. G. de Gennes, 1963, Solid State Commun. **1**, 132.

² R. Blinc and B. Zeks, 1974, Soft Modes in ferroelectrics and antiferroelectrics (North-holland, Amsterdam).

³ R. J. Elliott, G.A. Gekring, A. P. Malozemoff, S. P. Smith, N. S. Staude, and R. N. Tyte, 1971, J. Phys. C **4**, L179.

⁴ Y. L. Wang and B. Cooper, 1968, Phys. Rev. **172**, 539.

⁵ R. B. Stinchcombe, 1973, J. Phys. C **6**, 2459.

⁶ P. Pfeuty, 1970, Ann. Phy (N.Y) **57**, 79.

⁷ R. J. Elliott and I. D. Saville, 1974, J. Phys. C **7**, 3145.

⁸ A. B. Harris, 1974, J. Phys. C **7**, 3082.

⁹ R. B. Stinchcombe, 1981, J. Phys. C **14**, L263.

¹⁰ T. Yokota, 1988, J. Phys. C: Solid State Phys. **21**, 5987.

¹¹ F. C. Sà Barreto, I. P. Fittipaldi and B. Zeks, 1981, Ferroelectrics **39**, 1103.

¹² F. C. Sà Barreto and I. P. Fittipaldi, 1985, Physica A **129**, 360.

¹³ Chuan-Zhang Yang and Jia-Lin Zhong, 1989, Phys.Stat.Sol. (b) **153**, 323.

¹⁴ Jia-Lin Zhong, Jia-Liang Li and Chuang-Zhang Yang, 1990, Phys. Stat. Sol. (b) **160**, 329.

¹⁵ M. Saber and J. W. Tucker, 1991, J. Magn. Magn. Mater. **102**, 287.

¹⁶ I. P. Fittipaldi, E. F. Sarmento, T. Kaneyoshi, 1992, Physica A **186**, 591.

¹⁷ E. F. Sarmento, I. P. Fittipaldi and T. Kaneyoshi, 1992, J. Magn. Magn. Mater. **104-107**, 233.

¹⁸ J. W. Tucker, 1993, J. Magn. Magn. Mater. **119**, 161.

¹⁹ Song-Tas Dai and Qing Jiang, 1990, Phys. Rev.B **42**, 2597.

²⁰ J. Oitmaa and G. J. Coombs, 1981, J. Phys. C **14**, 143.

²¹ Yu qiang Ma and Chang-de Gong, 1992, J. Phys: Cond. Matter **4**, L313.

²² W. J. Song and C. Z. Yang, 1994, Phys.Stat.Sol.(b) **186**, 511.

²³ T. Kaneyoshi, M. Jascur and I. P. Fittipaldi, 1993, Phys. Rev. B **48**, 250.

²⁴ J. W. Tucker, M. Saber and H. Ez-Zahraoui, 1995, J. Magn. Magn. Mater **139**, 83. A. Elkouraychi, M. Saber and J.W. Tucker, 1995, Physica A **213**, 576.

²⁵ T. F. Cassol, W. Figueiredo and J. A. Plascak, 1991, Phys. Lett. A **160**, 518.

²⁶ W. J. Song, 1994, Solid State Commun. **89**, 379.

²⁷ W. J. Song, and C. Z. Yang, 1994, Solid State Commun. **92**, 361.

²⁸ Yong-qianq Wang and Zheng-ya Li, 1994, J. Phys.: Cond. Mater **6**, 10067.

²⁹ M. Suzuki, 1976, Prog. Theor. Phys. **56**, 1454.

- ³⁰ T. Yokota, 1992, Phys. Lett. A **171**, 134.
- ³¹ L. Néel, 1948, Ann. Phys. (Paris) **3**, 137.
- ³² M. Drillon, E. Coronado, D. Beltran and R. Georges, 1983, J. Chem. Phys. **79**, 449.
- ³³ S. L. Schofield and R. G. Bowers, 1980, J. Phys. A: Math. Gen. **13**, 3697.
- ³⁴ N. Benayad, 1990, Z. Phys. B: Cond. Matter **81**, 99.
- ³⁵ B. Y. Yousif and R. G. Bowers, 1984, J. Phys. A: Math. Gen. **17**, 3389.
- ³⁶ Kun-Fa Tang, 1988, J. Phys. A: Math. Gen. **21**, L1097.
- ³⁷ N. Benayad, A. Klümper, J. Zittartz and A. Benyoussef, 1989, Z. Phys. B: Cond. Matter **77**, 333; N. Benayad, A. Klümper, J. Zittartz and A. Benyoussef, 1989, Z. Phys. B: Cond. Matter **77**, 339.
- ³⁸ N. Benayad, A. Dakhama, A. Klümper and J. Zittartz, 1996, Ann. Physik **5**, 387.
- ³⁹ T. Kaneyoshi, E. F. Sarmiento and I. P. Fittipaldi, 1988, Phys. Stat. Sol.(b) **150**, 261.
- ⁴⁰ T. Kaneyoshi, 1995, Phys. Stat. Sol.(b) **189**, 219.
- ⁴¹ N. Benayad, A. Dakhama, A. Klümper and J. Zittartz, 1996, Z. Phys. B: Cond. Matter **101**, 623.
- ⁴² N. Benayad, A. Dakhama, A. Fathi and R. Zerhouni, 1998, J. Phys.: Cond. Matter **10**, 3141.
- ⁴³ J. W. Tucker, M. Saber, L. Peliti, 1994, Physica A **206**, 497.
- ⁴⁴ J. W. Tucker, 1994, J. Phys. A: Math. Gen. **27**, 659.
- ⁴⁵ J. W. Tucker, 1991, J. Magnetism. Magnetic Mater. **102**, 144.
- ⁴⁶ M. Kerouad, M. Saber and J. W. Tucker, 1993, Phys. Stat. Sol. (b) **180**, K23.
- ⁴⁷ N. Benayad and R. Zerhouni, 1997, Phys. Stat. Sol.(b) **201**, 491.
- ⁴⁸ M. F. Sykes and J. W. Essam, 1964, Phys. Rev. **133**, A 310.
- ⁴⁹ R. J. Elliott and I. D. Saville, 1974, J. Phys. C **7**, 4293.
- ⁵⁰ I. Tamura, E. F. Sarmiento and T. Kaneyoshi, 1984, J. Phys. C **17**, 3207.
- ⁵¹ E. J. S. Laje, 1976, D. Phyl. Thesis, Oxford University.
- ⁵² R. R. Santos, 1981, J. Phys. C **15**, 3141 (1982); J. Phys.A.**14**, L179.